JOURNAL OF COMPUTATIONAL PHYSICS 13, 316–337 (1973)

Hopscotch Methods for an Anisotropic Thermal Print Head Problem

JOHN LL. MORRIS AND IAN F. NICOLL

Department of Mathematics, University of Dundee, Dundee, Scotland

Received March 5, 1973

A class of hopscotch methods is considered for the solution of a heat equation with constant coefficients, defining the heat flow in a thermal print head. The behavior of the finite difference schemes for the numerical solution of the heat equation is studied for both isotropic and anisotropic media.

1. INTRODUCTION

The flow of heat in a thermal print head subject to a discontinuous heat source generated in a thin film deposited on the surface of a glass substrate was first considered in a paper by Chen [1]. An unusual feature of Chen's model was that the three-dimensional heat equation for the substrate required the solution of a two-dimensional heat equation for the thin film as one of the boundary conditions. The complex nature of the mathematical problem made a general analytical solution impossible. Thus, numerical analysis techniques played an important role in obtaining a solution to such a problem.

In [1] the partial differential equations for the heat flow were solved numerically by the implementation of an explicit finite difference scheme for the substrate problem and an implicit method for the thin film. However, the use of the explicit scheme was severely restricted by convergence criteria. In a paper by Morris [9] alternating direction and locally one-dimension methods (see Mitchell [8]) were applied to the solution of the problem of [1]. Such schemes required the solution of sets of simultaneous equations which was time consuming and restrictive on the size of problem to be solved.

Following original work by Gordon [4], (see also Saul'iev [13]), a fast algorithm for the solution of partial differential equations was developed by Gourlay [5]. The method was called the hopscotch algorithm because of the way the scheme progressed through the time–space grid. Later a more general class of hopscotch methods was introduced by Gourlay and McGuire [6]. The structure and properties of these algorithms made them particularly easy to implement. Recently Morris [10] adapted a hopscotch technique to a modified model of the original

thermal print head problem in which the physical heating element embedded in the thin film was replaced by an incident normal beam of electrons. Good computational results were obtained, and it was concluded that the hopscotch scheme was a very attractive method to use for the solution of complicated physical problems.

Up until this point the discussions with regard to the heat flow in a thermal print head have been restricted to considering the substrate and thin film as isotropic media. (A homogeneous solid is said to be isotropic if it is of such material that when a point within it is heated, the heat spreads out equally in all directions.) When certain directions are more favorable for the conduction of heat than others then the medium is said to be anisotropic. However, finite difference methods used to date are unsatisfactory for anisotropic partial differential equations in that poor accuracy is achieved in practice.

Recently some techniques have been produced which improve the accuracy of the results. Watts [11, 12] presented a method which required an iterated solution of a system of simultaneous linear equations. A line successive over-relaxation (L.S.O.R.) technique was used with the columns orientated in the direction of high conductivity. A column correction process requiring the solution of a tridiagonal set of equations was implemented after a number of L.S.O.R. sweeps to bring the solution vector closer to its correct values. Such a scheme, however, was slower than any available method for the solution of isotropic problems and was only applicable to equilibrium problems.

Chu, Morton, and Roberts [3] and Chu and Johannson [2] investigated the numerical solution of the anisotropic heat conduction equation in which the axes of the finite difference grid were at an angle to the principal axes of conductivity. The authors endeavored to solve the problem of the anisotropy by transforming the anisotropic partial differential equation into a nonanisotropic partial differential equation by a rotation of axes. In this case a cross derivative term was introduced, and the authors considered finite difference methods for this equation. We will adopt the alternative strategy of considering the original partial differential equation per se and consider the properties of the class of hopscotch methods as described in [6].

In Section 2 we briefly describe the physical problem and define the mathematical model. The hopscotch schemes are outlined and analyzed with respect to the anisotropic terms in Section 3. In Section 4 the computational results for several numerical experiments are reported. The paper is concluded in Section 5.

2. The Physical Problem and Its Associated Mathematical Formulation

A thermal print head is composed of a glass substrate surmounted by a thin film of a material with high thermal conductivity properties. Embedded in the thin film

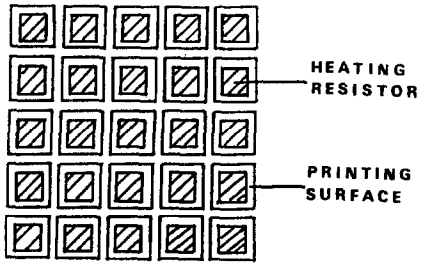

FIG. 1. A 5 × 5 matrix thermal print head (top view).

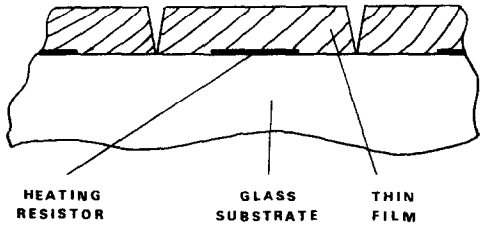

FIG. 2. A single element of the matrix (side view).

layer is a matrix of heat resistors (Figs. 1 and 2). When a current is passed through the resistors their immediate neighborhood is heated. When heat is applied to a thermally sensitive paper, a chemical reaction will occur if the heat induces a temperature above a certain threshold. By heating specific elements in the matrix, characters can be produced on the paper. When the current is switched off, the glass substrate acts as a heat sink allowing the printing surface to cool rapidly.

This printing technique can be made faster than conventional mechanical devices if an optimal "time on/time off" cycle for the current in the thermal print head can be found. In addition the physical properties of the materials used in the manufacture of the thermal print head need to be considered carefully. For a given set of physical parameters, a given on–off switching of the heat source can cause an overall rise in the print head temperature which in turn results in indistinct characters being produced on the print paper. In this case it is likely that the off-time between each character-printing would have to be increased thereby slowing down the print cycle.

In our investigation several numerical simulations of the thermal print head are made for varying physical constants and in particular those which give rise to anisotropy.

The mathematical model [1] assumes that the thickness of the thin film is so small in comparison with that of the glass substrate, and the thermal conductivity

coefficient for the thin film to be sufficiently high so as to make the temperature gradient in the vertical direction negligible. If we represent the vertical direction in a Cartesian coordinate system (x, y, z, t) by z, this effectively means that the thin film has no dimension in the z coordinate other than to give it a thermal capacity due to a thickness D of the thin film, say.

The heat equation governing the heat distribution in the thin film is then

$$\frac{\partial u}{\partial t} = \frac{\kappa_1}{\rho C}\frac{\partial^2 u}{\partial x^2} + \frac{\kappa_2}{\rho C}\frac{\partial^2 u}{\partial y^2} + \frac{s(x, y, t)}{\rho C} - \frac{h_0}{D\rho C}(u - u_\infty), \tag{1}$$

where $u = u(x, y, 0, t)$ denotes the temperature in degrees centigrade at a point $(x, y, 0, t)$ in the thin film. κ_1 is the thermal conductivity of the thin film in the x direction, κ_2 is the corresponding thermal conductivity in the y direction, ρ is the density, C is the specific heat, u_∞ is the ambient temperature, and h_0 is the convective heat transfer coefficient between the thin film and air. The term,

$$\begin{aligned} s(x, y, t) = &\left\{1 - \sum_{i=0}^{2n-2} (-1)^i H(t - t_i)\right\} \\ &\times \left\{\sum_{j=0}^{m-1}\sum_{k=0}^{m-1} [H(x - j\beta - \alpha) - H(x - (j+1)\beta + \alpha)]\right. \\ &\left.\times [H(y - k\beta - \alpha) - H(y - (k+1)\beta + \alpha)]\right\}, \end{aligned}$$

where $H(\theta)$ is the Heaviside function defined by

$$H(\theta) = \begin{cases} 0 & \theta < 0, \\ 1 & \theta > 0, \end{cases}$$

represents a heat source with discontinuous in both time and space for a print head composed of an $m \times m$ matrix of heating elements with n on-off switches. The t_i are defined such that t_i, $i = 0, 2, 4, \ldots, 2n - 2$, are the switch-off times and t_i, $i = 1, 3, 5, \ldots, 2n - 3$, are the switch-on times for the heat source. The heat resistors are defined as the squares

$$\{(x, y): j\beta + \alpha \leqslant x \leqslant (j+1)\beta - \alpha, k\beta + \alpha \leqslant y \leqslant (k+1)\beta - \alpha, 0 \leqslant j, k \leqslant m-1\},$$

where β is the side length of a single print element, and q is the heat generated in watts per unit volume.

The initial condition $u(x, y, 0, 0) = f(x, y, 0)$, $0 \leqslant x, y \leqslant l$ and the boundary conditions $\partial u/\partial \eta = 0$, $x = 0, l$; $0 \leqslant y \leqslant l$, $y = 0, l$; $0 \leqslant x \leqslant l$ are given for Eq. (1) where $l = m \times \beta$ is the overall side length of the print head, η is the

outward drawn normal to the edges of the thin film, and f is a continuous function. We assume continuity of initial and boundary conditions.

In the forthcoming section, for simplicity of analysis, we will consider only a single heat element. We will further assume that the heat resistor covers the entire upper surface of the print head, i.e., $\alpha = 0$. The case in which the heat source is discontinuous in space ($\alpha > 0$) as well as in time will be considered in a later paper.

The region in which the solution is required is defined by,

$$\bar{R} = R \times [0 < t \leqslant T],$$

where $R = \{(x, y, z); 0 < x, y, z < \beta\}$ and we denote the boundary of $\bar{R}$ by $\partial\bar{R}$ so that the solution of Eq. (1), with initial conditions and boundary conditions, constitutes a boundary condition on $\partial\bar{R}_{z=0}$ for the total print head.

The equation governing the temperature distribution u in the glass substrate is

$$\frac{\partial u}{\partial t} = \frac{\kappa_3}{\rho_1 C_1}\frac{\partial^2 u}{\partial x^2} + \frac{\kappa_4}{\rho_1 C_1}\frac{\partial^2 u}{\partial y^2} + \frac{\kappa_5}{\rho_1 C_1}\frac{\partial^2 u}{\partial z^2} \tag{2}$$

subject to the initial condition

$$u(x, y, z, 0) = f(x, y, z) \qquad 0 \leqslant x, y, z \leqslant \beta$$

and the boundary conditions

$$\partial u/\partial\eta = 0 \qquad \text{on} \qquad \partial\bar{R}_{x=0,\beta} \qquad \text{and} \qquad \partial\bar{R}_{y=0,\beta},$$

$u(x, y, \beta, t) = g(x, y, \beta, t)$ and $u(x, y, 0, t)$ is the solution of Eqs. (1) and (2) on $\partial\bar{R}_{z=\beta,0}$, respectively. κ_3, κ_4, κ_5 are the conductivity coefficients of the substrate in the x, y, and z directions, respectively, ρ_1, is the density, and C_1 is the specific heat. The print head has been assumed to be a cube for programing convenience; the results are easily extendible to any rectangular shaped print head.

3. The Numerical Methods

In this section we shall consider the odd–even hopscotch, line hopscotch, and A.D.I. hopscotch difference schemes [6, 7] for the numerical solution of Eqs. (1) and (2) with their respective initial/boundary conditions.

A rectilinear grid is superimposed on the region of computation $\bar{R}$ where the mesh spacings in the space variables are taken equal; namely

$$\Delta_x = \Delta_y = \Delta_z = h,$$

and the mesh spacing in the time dimension Δ_t is denoted by τ. The mesh ratio $r = \tau/h^2$ is taken to be constant throughout. We denote by u_{ijk}^m the value of the unknown u at the point $(ih, jh, kh, \tau m) = (x, y, z, t)$ $i, j, k = 0, 1, \ldots, N$, $Nh = \beta$, and $m = 0, 1, 2, \ldots$.

We will use the central difference operators,

$$\delta_x u_{ijk}^m = u_{(i+\frac{1}{2})jk}^m - u_{(i-\frac{1}{2})jk}^m$$

with similar expressions for δ_y and δ_z .

We will write Eq. (1) in the form

$$\partial u/\partial t = Lu + d(x, y, t), \tag{3}$$

where $L = a(\partial^2/\partial x^2) + b(\partial^2/\partial y^2) + c$ is a linear elliptic differential operator and

$$a = \kappa_1/\rho C, \qquad b = \kappa_2/\rho C, \qquad c = -h_0/D\rho C,$$
$$d(x, y, t) = s(x, y, t)/\rho C + h_0 u_\infty/D\rho C.$$

The general hopscotch scheme for Eq. (3) is given by

$$\begin{aligned} u_{ij}^{m+1} - \tau(\theta_{ij}^{m+1} L_h^{(1)} + \eta_{ij}^{m+1} L_h^{(2)})\, u_{ij}^{m+1} &= u_{ij}^m + \tau(\theta_{ij}^m L_h^{(1)} + \eta_{ij}^m L_h^{(2)})\, u_{ij}^m \\ &\quad + \tau(\theta_{ij}^{m+1} d_{ij}^{(1)m+1} + \eta_{ij}^{m+1} d_{ij}^{(2)m+1}) \\ &\quad + \tau(\theta_{ij}^m d_{ij}^{(1)m} + \eta_{ij}^m d_{ij}^{(2)m}) \\ d_{ij}^{(1)m} + d_{ij}^{(2)m} &= d_{ij}^m \end{aligned} \tag{4}$$

with the restrictions

$$\theta_{ij}^{m+1} + \theta_{ij}^m = 1,$$
$$\eta_{ij}^{m+1} + \eta_{ij}^m = 1.$$

$L_h \equiv L_h^{(1)} + L_h^{(2)}$ is the finite difference replacement for the differential operator $L \equiv L^{(1)} + L^{(2)}$ where $L^{(1)}$ and $L^{(2)}$ are one-dimensional operators, namely $L^{(1)} = a(\partial^2/\partial x^2) + c_1$ and similarly $L^{(2)} = b(\partial^2/\partial y^2) + c_2$ with $c = c_1 + c_2$. $L_h^{(1)}$ and $L_h^{(2)}$ can be any consistent E-operators (in the sense of [5]). However, to be precise, we will assume the simplest difference replacements of $L^{(1)}$ and $L^{(2)}$ given by

$$L_h^{(1)} \equiv (a/h^2)\, \delta_x^{\,2} + c_1 = L^{(1)} + o(h^2),$$
$$L_h^{(2)} \equiv (b/h^2)\, \delta_y^{\,2} + c_2 = L^{(2)} + o(h^2).$$

Defining

$$\theta_{ij}^m = \eta_{ij}^m = \begin{cases} 1 & i + j + m \text{ even}, \\ 0 & i + j + m \text{ odd}, \end{cases}$$

we obtain the odd-even hopscotch method

$$u_{ij}^{m+1} - \tau\theta_{ij}^{m+1}L_h u_{ij}^{m+1} = u_{ij}^m + \tau\theta_{ij}^m L_h u_{ij}^m + \tau(\theta_{ij}^{m+1}d_{ij}^{m+1} + \theta_{ij}^m d_{ij}^m) \tag{5}$$

or

$$u_{ij}^{m+1} = u_{ij}^m + \tau L_h u_{ij}^m + \tau d_{ij}^m \qquad i + j + m \text{ even}, \tag{6}$$

$$u_{ij}^{m+1} - \tau L_h u_{ij}^{m+1} = u_{ij}^m + \tau d_{ij}^{m+1} \qquad i + j + m \text{ odd}. \tag{7}$$

The computational algorithm proceeds as in [5] the details of which are omitted here.

Writing Eq. (5) over two time steps and eliminating the term $\theta_{ij}^{m+1}L_h u_{ij}^{m+1}$ we obtain

$$u_{ij}^{m+2} - \tau\theta_{ij}^m L_h(u_{ij}^{m+2} + u_{ij}^m) = 2u_{ij}^{m+1} - u_{ij}^m . \tag{8}$$

When θ_{ij}^m is zero, Eq. (8) reduces to the explicit scheme

$$u_{ij}^{m+2} = 2u_{ij}^{m+1} - u_{ij}^m ,$$

and, consequently, for half the points an extremely simple substitution attains the approximation required at the next time level. Full details of the implementation of this fast odd–even hopscotch algorithm are given in [5].

The local truncation error for the odd–even hopscotch scheme with the difference operator $L_h = (a/h^2)\,\delta_x^2 + (b/h^2)\,\delta_y^2 + c$ is obtained as follows: Writing Eqs. (6) and (7) such that $i + j + m$ is even in both cases and expanding L_h we obtain

$$u_{ij}^{m+1} = (1 - 2ar - 2br + \tau c)\,u_{ij}^m + ar(u_{i+1j}^m + u_{i-1j}^m) + br(u_{ij+1}^m + u_{ij-1}^m) + \tau d_{ij}^m , \tag{9}$$

$$(1 + 2ar + 2br - \tau c)\,u_{ij}^m = u_{ij}^{m\ 1} + ar(u_{i+1j}^m + u_{i-1j}^m) + br(u_{ij+1}^m + u_{ij-1}^m) + \tau d_{ij}^m . \tag{10}$$

Eliminating the u_{ij}^m term from Eqs. (9) and (10) gives

$$(1 + 2ar + 2br - \tau c)\,u_{ij}^{m+1} = (1 - 2ar - 2br + \tau c)\,u_{ij}^{m-1} + 2ar(u_{i+1j}^m + u_{i-1j}^m) + 2br(u_{ij+1}^m + u_{ij-1}^m) + 2\tau d_{ij}^m . \tag{11}$$

A Taylor series expansion gives

$$\frac{\partial u}{\partial t} + (2ar + 2br - \tau c)\frac{\tau}{2}\frac{\partial^2 u}{\partial t^2} = a\frac{\partial^2 u}{\partial x^2} + b\frac{\partial^2 u}{\partial y^2} + cu + d + \frac{h^2}{12}\left(a\frac{\partial^4 u}{\partial x^4} + b\frac{\partial^4 u}{\partial y^4}\right) + o(\tau^2 + h^4).$$

Therefore, the principal part of the local truncation error is

$$(2ar + 2br - \tau c)\frac{\tau}{2}\frac{\partial^2 u}{\partial t^2} - \frac{h^2}{12}\left(a\frac{\partial^4 u}{\partial x^4} + b\frac{\partial^4 u}{\partial y^4}\right). \tag{12}$$

Defining

$$\theta_{ij}^m = \eta_{ij}^m = \begin{cases} 1 & i + m \text{ even}, \\ 0 & i + m \text{ odd} \end{cases} \tag{13}$$

gives another hopscotch method.

$$u_{ij}^{m+1} = u_{ij}^m + \tau L_h u_{ij}^m + \tau d_{ij}^m \qquad i + m \text{ even}, \tag{14}$$

$$u_{ij}^{m+1} - \tau L_h u_{ij}^{m+1} = u_{ij}^m + \tau d_{ij}^m \qquad i + m \text{ odd}. \tag{15}$$

It is easily seen that this algorithm requires the solution of a tridiagonal system of equations to obtain approximate values at points along alternating i-grid lines, i.e., in the y direction. The above method is called the line hopscotch scheme. Similarly defining

$$\theta_{ij}^m = \eta_{ij}^m = \begin{cases} 1 & j + m \text{ even}, \\ 0 & j + m \text{ odd} \end{cases}$$

produces a line hopscotch algorithm with the implicit scheme orientated along the x direction.

On replacing the θ_{ij}^m in Eq. (8) by that defined in Eq. (13) it is easily seen that a fast line hopscotch can be obtained.

Writing Eqs. (14) and (15) for $i + m$ even and eliminating the u_{ij}^m terms leads to the equation

$$\begin{aligned}(1 + 2ar - br\delta_y^2 - \tau c)\, u_{ij}^{m+1} \\ = 2ar(u_{i+1j}^m + u_{i-1j}^m) + (1 - 2ar + br\delta_y^2 + \tau c)\, u_{ij}^{m-1} + 2\tau d_{ij}^m .\end{aligned} \tag{16}$$

Taylor series expansion gives

$$\begin{aligned}\frac{\partial u}{\partial t} + (2ar - \tau c)\frac{\tau}{2}\frac{\partial^2 u}{\partial t^2} - \frac{b\tau^2}{2}\frac{\partial^4 u}{\partial t^2\, \partial y^2} \\ = a\frac{\partial^2 u}{\partial x^2} + b\frac{\partial^2 u}{\partial y^2} + cu + d + \frac{h^2}{12}\left(a\frac{\partial^4 u}{\partial x^4} + b\frac{\partial^4 u}{\partial y^4}\right) + o(\tau^2 + h^4).\end{aligned}$$

The principal part of the line hopscotch truncation error is, therefore,

$$(2ar - \tau c)\frac{\tau}{2}\frac{\partial^2 u}{\partial t^2} - \frac{b\tau^2}{2}\frac{\partial^4 u}{\partial t^2\, \partial y^2} - \frac{h^2}{12}\left(a\frac{\partial^4 u}{\partial x^4} + b\frac{\partial^4 u}{\partial y^4}\right). \tag{17}$$

When

$$\theta_{ij}^m = \eta_{ij}^{m+1} = \begin{cases} 1 & i+m \text{ even}, \\ 0 & i+m \text{ odd} \end{cases}$$

we have the A.D.I. hopscotch scheme

$$\begin{aligned} u_{ij}^{m+1} - \tau(\theta_{ij}^{m+1} L_h^{(1)} + \theta_{ij}^m L_h^{(2)})\, u_{ij}^{m+1} &= u_{ij}^m + \tau(\theta_{ij}^m L_h^{(1)} + \theta_{ij}^{m+1} L_h^{(2)})\, u_{ij}^m \\ &\quad + \tau(\theta_{ij}^{m+1} d_{ij}^{(1)m+1} + \theta_{ij}^m d_{ij}^{(2)m+1}) \\ &\quad + \tau(\theta_{ij}^m d_{ij}^{(1)m} + \theta_{ij}^{m+1} d_{ij}^{(2)m}) \end{aligned} \tag{18}$$

or

$$(1 - \tau L_h^{(2)})\, u_{ij}^{m+1} = (1 + \tau L_h^{(1)})\, u_{ij}^m + \tau(d_{ij}^{(2)m+1} + d_{ij}^{(1)m}) \qquad i+m \text{ even}, \tag{19}$$

$$(1 - \tau L_h^{(1)})\, u_{ij}^{m+1} = (1 + \tau L_h^{(2)})\, u_{ij}^m + \tau(d_{ij}^{(1)m+1} + d_{ij}^{(2)m}) \qquad i+m \text{ odd}. \tag{20}$$

With the above three point replacements for $L_h^{(1)}$ and $L_h^{(2)}$ Eq. (19) requires the solution of a tridiagonal system of equations along alternate i-grid lines, and, therefore, Eq. (20) now becomes an explicit process.

Similar analysis to that for the truncation error for the line hopscotch method gives for the truncation error of the A.D.I. scheme

$$\begin{aligned} &(\tau c_1 - 2ar)\,\tau c_2 \frac{\partial u}{\partial t} + (2ar - \tau c)\frac{\tau}{2}\frac{\partial^2 u}{\partial t^2} + b(\tau c_1 - 2ar)\tau \frac{\partial^3 u}{\partial t\, \partial y^2} \\ &- \frac{b\tau^2}{2}\frac{\partial^4 u}{\partial t^2\, \partial y^2} + (\tau c_1 - 2ar)\tau \frac{\partial d^{(2)}}{\partial t} - \frac{\tau^2}{2}\frac{\partial^2 d^{(2)}}{\partial t^2} - \frac{h^2}{12}\left(a\frac{\partial^4 u}{\partial x^4} + b\frac{\partial^4 u}{\partial y^4}\right). \end{aligned} \tag{21}$$

Therefore, we must choose $d^{(2)} = 0$, $d^{(1)} = d$ to eliminate the time derivatives of a Heaviside function from the analysis.

The form of the principal truncation errors, Eqs. (12), (17), and (21), is to prove crucial in the application of the hopscotch methods for the anisotropic problems.

Consider Eq. (12); here the truncation error contains $o(\tau)$ terms dependent upon both of the diffusivity coefficients a and b. Consequently, the direction of anisotropy is not going to prove significant for this method since the error term will contain a substantially large anisotropic coefficient. This in turn will be mirrored by relatively large errors in the computed solutions.

In contrast, the principal truncation error Eq. (17) of the line hopscotch method contains an $o(\tau)$ term involving just the diffusivity coefficient a when the implicit scheme is orientated along the direction of the x-axis. To propose the line hopscotch scheme with the direction of the implicit scheme orientated along the y-axis will clearly replace the coefficient a by b in the $o(\tau)$ term (together with the obvious changes in the remaining terms). In this case however, if one coefficient is large

relative to the other, it will be important which of the two possible line hopscotch schemes is used. For example, if a is small relative to b then the scheme as proposed by Eqs. (14) and (15) should produce significantly more accurate results than its complement scheme.

Similarly in considering the principal truncation error of the A.D.I. hopscotch scheme given by Eq. (21), we find once again that just one diffusivity coefficient appears in the $o(\tau)$ part of the principal truncation error. For the same reasons outlined above, the direction of the implicit scheme in the A.D.I. hopscotch method should be chosen so that this coefficient is the smaller of the two, that is the direction of the implicit scheme should be chosen parallel to the direction of anisotropy.

The above hopscotch algorithms can easily be extended to solve numerically the three-dimensional heat equation (2) which can be written in the form

$$\frac{\partial u}{\partial t} = Lu \qquad \text{where} \quad L = a\frac{\partial^2}{\partial x^2} + b\frac{\partial^2}{\partial y^2} + c\frac{\partial^2}{\partial z^2}$$

and

$$a = \frac{\kappa_3}{\rho_1 C_1}, \qquad b = \frac{\kappa_4}{\rho_1 C_1}, \qquad c = \frac{\kappa_5}{\rho_1 C_1}.$$

We define the finite difference operator

$$L_h = L_h^{(1)} + L_h^{(2)} = \frac{a}{h^2}\delta_x^{\,2} + \frac{b}{h^2}\delta_y^{\,2} + \frac{c}{h^2}\delta_z^{\,2}$$

which is split such that

$$L_h^{(1)} = \frac{a}{h^2}\delta_x^{\,2} + \frac{c}{h^2}\delta_z^{\,2} \qquad \text{and} \qquad L_h^{(2)} = \frac{b}{h^2}\delta_y^{\,2}.$$

The general three-dimensional hopscotch scheme is

$$u_{ijk}^{m+1} - \tau(\theta_{ijk}^{m+1}L_h^{(1)} + \eta_{ijk}^{m+1}L_h^{(2)})\,u_{ijk}^{m+1} = u_{ijk}^{m} + \tau(\theta_{ijk}^{m}L_h^{(1)} + \eta_{ijk}^{m}L_h^{(2)})\,u_{ijk}^{m}. \quad (22)$$

$$\theta_{ijk}^{m} = \eta_{ijk}^{m} = \begin{cases} 1 & \text{for} \quad i+j+k+m \text{ even}, \\ 0 & \text{for} \quad i+j+k+m \text{ odd}, \end{cases}$$

gives the odd–even hopscotch scheme

$$u_{ijk}^{m+1} = u_{ijk}^{m} + \tau L_h u_{ijk}^{m} \qquad \text{for} \quad i+j+k+m \text{ even}, \quad (23)$$

$$u_{ijk}^{m+1} - \tau L_h u_{ijk}^{m+1} = u_{ijk}^{m} \qquad \text{for} \quad i+j+k+m \text{ odd}, \quad (24)$$

with truncation error

$$(a+b+c)r\,\tau\frac{\partial^2 u}{\partial t^2}-\frac{h^2}{12}\left(a\frac{\partial^4 u}{\partial x^4}+b\frac{\partial^4 u}{\partial y^4}+c\frac{\partial^4 u}{\partial z^4}\right)+o(\tau^2+h^4). \tag{25}$$

Defining

$$\theta_{ijk}^m=\eta_{ijk}^m=\begin{cases}1 & i+k+m \text{ even},\\ 0 & i+k+m \text{ odd},\end{cases}$$

we obtain a line hopscotch algorithm in three dimensions.

$$u_{ijk}^{m+1}=u_{ijk}^m+\tau L_h u_{ijk}^m \qquad \text{for } i+k+m \text{ even}, \tag{26}$$

$$u_{ijk}^{m+1}-\tau L_h u_{ijk}^{m+1}=u_{ijk}^m \qquad \text{for } i+k+m \text{ odd}, \tag{27}$$

with truncation error

$$ar\,\tau\frac{\partial^2 u}{\partial t^2}-\frac{\tau^2}{2}\left(b\frac{\partial^4 u}{\partial t^2\,\partial y^2}+c\frac{\partial^4 u}{\partial t^2\,\partial z^2}\right)-\frac{h^2}{12}\left(a\frac{\partial^4 u}{\partial x^4}+b\frac{\partial^4 u}{\partial y^4}+c\frac{\partial^4 u}{\partial z^4}\right). \tag{28}$$

Finally

$$\theta_{ijk}^m=\eta_{ijk}^{m+1}=\begin{cases}1 & \text{for } i+k+m \text{ even},\\ 0 & \text{for } i+k+m \text{ odd},\end{cases}$$

gives a three-dimensional A.D.I. type scheme

$$(1-\tau L_h^{(2)})\,u_{ijk}^{m+1}=(1+\tau L_h^{(1)})\,u_{ijk}^m \qquad \text{for } i+k+m \text{ even}, \tag{29}$$

$$(1-\tau L_h^{(1)})\,u_{ijk}^{m+1}=(1+\tau L_h^{(2)})\,u_{ijk}^m \qquad \text{for } i+k+m \text{ odd}, \tag{30}$$

where the truncation error is given by

$$ar\,\tau\frac{\partial^2 u}{\partial t^2}-\frac{\tau^2}{2}\left(b\frac{\partial^4 u}{\partial t^2\,\partial y^2}+c\frac{\partial^4 u}{\partial t^2\,\partial z^2}\right)-\frac{h^2}{12}\left(a\frac{\partial^4 u}{\partial x^4}+b\frac{\partial^4 u}{\partial y^4}+c\frac{\partial^4 u}{\partial z^4}\right). \tag{31}$$

Our remarks regarding the orientation of the implicit portion of the schemes for the two-dimensional hopscotch schemes are clearly relevant once again here, where we assume a unidirectional anisotropy (the case of two directions of anisotropy will be considered in a future paper). The normal boundary conditions are applied by using the simple difference replacements $\partial u/\partial x\,|_{x=0}=(u_{1jk}^m-u_{-1jk}^m)/2h$ and $\partial u/\partial x\,|_{x=\beta}=(u_{(N+1)jk}^m-u_{(N-1)jk}^m)/2h$ with similar expressions for $\partial u/\partial y\,|_{y=0}$ and $\partial u/\partial y\,|_{y=\beta}$, and, therefore, by the nature of the hopscotch schemes no boundary

4. Numerical Results

A series of experiments was carried out to test the hopscotch schemes, outlined in Section 3, for the numerical solution of the thermal print head model in both isotropic and anisotropic media.

Assuming the heat source to be constant ($t_0 = \infty$) and with the additional restrictions $\alpha = 0$, $u_\infty = 0$, $u(x, y, \beta, t) = g(x, y, \beta, t) = 0$ for all time, a theoretical solution to Eqs. (1) and (2) with associated initial/boundary conditions can be obtained, namely,

$$u = \left(e^{\gamma t} \cos \frac{\pi x}{l} \cos \frac{\pi y}{l} + \frac{Dq}{h_0}\right)\left(1 - \frac{z}{l}\right) + e^{\lambda t} \cos \frac{\pi x}{l} \cos \frac{\pi y}{l} \sin \frac{\pi z}{l}, \quad (32)$$

where

$$\gamma = -\frac{\pi^2(\kappa_3 + \kappa_4)}{l^2 \rho_1 C_1}, \qquad \lambda = -\frac{\pi^2(\kappa_3 + \kappa_4 + \kappa_5)}{l^2 \rho_1 C_1},$$
$$D = \frac{h_0 l^2}{\rho C((\kappa_3 + \kappa_4)/\rho_1 C_1 - (\kappa_1 + \kappa_2)/\rho C)}. \quad (33)$$

To obtain a positive value for the thin film thickness D we are restricted to making the diffusivity of the substrate greater than that of the thin film. Therefore, although the solution (32) to the print head model is not physically reasonable we are able to obtain comparisons of the hopscotch methods and also determine their accuracy.

It is to be noted that no theoretical solution covering the whole print head is known for a discontinuous heat source. However, a theoretical solution can be obtained for a single heat element thin film equation in which there is a single on-off switching namely, the heat source initially on, is switched off after t_0 sec.

With $\alpha = 0$ and $u_\infty = 0$ the solution to Eq. (1) is

$$u = \frac{Dq}{h_0}(1 - e^{\nu(t\ t_0)})(1 - H(t - t_0)) + \cos \frac{\pi x}{\beta} \cos \frac{\pi y}{\beta} e^{(\nu+\gamma)t}, \quad (34)$$

where

$$\nu = -\frac{h_0}{D\rho C} \quad \text{and} \quad \gamma = -\frac{\pi^2(\kappa_1 + \kappa_2)}{\beta^2 \rho C}.$$

The theoretical solution for the discontinuous heat source problem provides a further means of testing the hopscotch schemes.

Isotropic Problems for a Single Element

In order to obtain a basis for comparison for the methods under the assumptions of anisotropy, we first considered the results obtained by the hopscotch methods

on isotropic problems. To obtain an estimate of the accuracy in this case (and to ensure the programs were completely debugged) the heat problem, for which a theoretical solution is known, was solved first. The values of the isotropic parameters used are as follows $h = 1/10$, $\kappa_1 = \kappa_2 = 0.5$, $\rho = 24.42$, $C = 2.6$, $\kappa_3 = \kappa_4 = \kappa_5 = 0.005$, $\rho_1 = 0.12$, $C_1 = 3.0095$, $h_0 = 0.000679$, $D = 0.00011045$ (from Eq. (33)), $u_\infty = 0$, $q = 10$.

The results obtained using the hopscotch methods are indicated in Table I. We would expect, as a result of the analysis of the principal truncation errors, that the numerical errors (the difference between the theoretical and computed solutions) would be of the same order of magnitude. This is clearly confirmed by the results of Table I.

TABLE I

Maximum Absolute Error at 100 Time Steps in the Print Head

r	Odd–even	Line	A.D.I.
0.1	4.050×10^{-4}	4.050×10^{-4}	4.051×10^{-4}
0.3	1.134×10^{-3}	1.134×10^{-3}	1.135×10^{-3}
0.6	2.039×10^{-3}	2.043×10^{-3}	2.050×10^{-3}
1.0	2.937×10^{-3}	2.952×10^{-3}	2.979×10^{-3}

It is to be noted that an increase of the value of the heat source by a factor ξ, say, brings about a corresponding increase in both the theoretical and computational solutions and, thus, variations in the heat source term have been omitted.

To investigate the effect of the discontinuous heat source upon the numerical results, the problem for which a theoretical solution is known in the thin film only, was also solved. The physical parameters used were the same as for the previous example. The maximum errors are quoted in Tables II and III. The result of the discontinuity is to increase the size of the errors by a factor of ten just after the switch off as compared with the errors just before the switch off. However, these errors do not grow for increasing time but remain of the same order of magnitude.

TABLE II

Maximum Absolute Error at 50 Time Steps in the Thin Film

r	Odd–even	Line	A.D.I.
0.1	6.291×10^{-5}	6.292×10^{-5}	6.292×10^{-5}
0.3	1.839×10^{-4}	1.840×10^{-4}	1.841×10^{-4}
0.6	3.534×10^{-4}	3.539×10^{-4}	3.545×10^{-4}
1.0	5.577×10^{-4}	5.594×10^{-4}	5.618×10^{-4}

TABLE III

Maximum Absolute Error at 100 Time Steps in the Thin Film

r	Odd–Even	Line	A.D.I.
0.1	2.542×10^{-4}	2.637×10^{-4}	2.698×10^{-4}
0.3	6.635×10^{-4}	7.170×10^{-4}	7.343×10^{-4}
0.6	1.163×10^{-3}	1.269×10^{-3}	1.301×10^{-3}
1.0	1.745×10^{-3}	1.861×10^{-3}	1.911×10^{-3}

As we mentioned above the set of parameters used in order that a theoretical solution can be obtained may be regarded as nonphysical. To test the hopscotch methods on a realistic isotropic problem the following set of parameters was chosen for a silver thin film surmounting a glass substrate, i.e., $\alpha = 0$, $\beta = l = 1$, $h = 1/10, r = 1.0, \kappa_1 = \kappa_2 = 1.0, \rho = 10.49, C = 0.0556, \kappa_3 = \kappa_4 = \kappa_5 = 0.0028$, $\rho_1 = 2.4$, $C_1 = 0.2$, $h_0 = 0.000053$, $u_\infty = 0$, $D = 0.000015$, $q = 10.0$. It is to be noted that for a discontinuous heat source no theoretical solution is known for the print head problem under the above conditions.

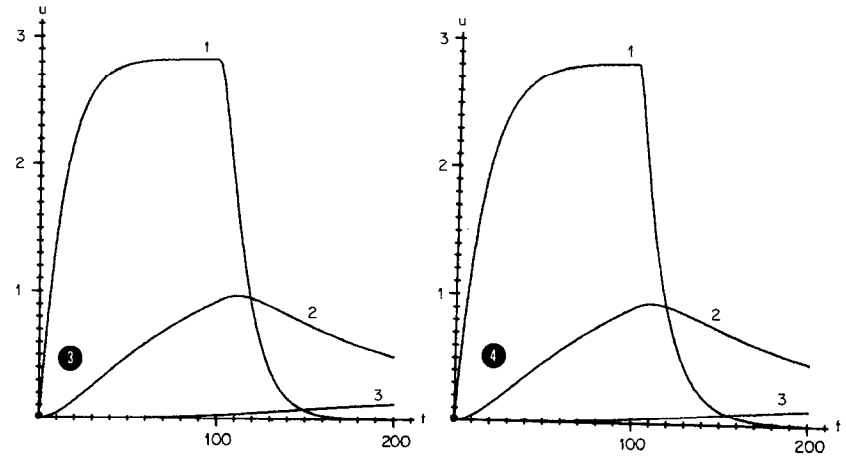

FIG. 3. Graphs[1] of temperature distribution in an isotropic thermal print element for a single switch off of the heat source; the solution obtained using the odd–even hopscotch algorithm.

FIG. 4. Graphs of temperature distribution in an isotropic thermal print element for a single switch off of the heat source; the solution obtained using the line hopscotch algorithm.

[1] In Figs. 3–15, graphs 1, 2, and 3 denote the temperature distributions in the thin film, and first and third substrate layers, respectively.

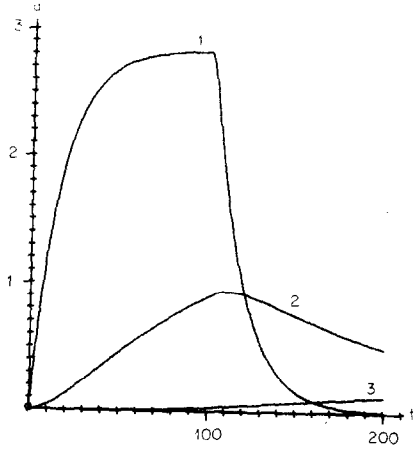

FIG. 5. Graphs of temperature distribution in an isotropic thermal print element for a single switch off of the heat source; the solution obtained using the A.D.I. hopscotch algorithm.

The print element was examined for a single switching of the heat source where $t_0 = 100\tau$. Graphs in Figs. 3–5 represent the temperature distribution at a fixed point ($x = y = 0.5$) and for $z = 0.0$, 0.1, and 0.3 where $0 \leqslant t \leqslant 200\tau$ as computed by the odd–even, line, and A.D.I. hopscotch methods, respectively.

Consideration of the solutions obtained in Figs. 3–5 indicates that there is little to choose between the three variants of the hopscotch method for the isotropic problem. The numerical results agree with the results previously reported in [9] using A.D.I. and L.O.D. methods. The amount of computation, however, represented by Figs. 3–5 is substantially less than that required in [9]. We have quoted just one of the variants of the possible line and A.D.I. hopscotch schemes, the results using the other variants were (obviously) precisely the same.

Anisotropic Problems for a Single Element

The computational experiments for the isotropic problems were repeated using the following physical constants $\alpha = 0, \beta = l = 1, h = 1/10, \kappa_1 = 1.0, \kappa_2 = 100.0, \rho = 15.154, C = 2.664, \kappa_3 = 0.005, \kappa_4 = 100.0, \kappa_5 = 0.005, \rho_1 = 6.5, C_1 = 6.019, h_0 = 0.000679, D = 0.00003936, u_{\infty} = 0, q = 10$. The print head is, therefore, highly anisotropic in the y direction.

Both the line and A.D.I. hopscotch schemes were implemented such that they were aligned with the direction of implicitness in the hopscotch scheme (a) perpendicular to the anisotropy and (b) parallel to the anisotropy.

As a result of the anisotropy the theoretical solution in both the continuous and discontinuous heat source problems (32) and (34) reach a steady state after only

a few time steps. For this reason we have only considered a comparison of the computational errors in the continuous heat source problem after ten time steps (Table IV) and for a ten steps on/ten steps off period for the discontinuous problem (Tables V and VI).

TABLE IV

Maximum Absolute Error at 10 Time Steps in the Print Head

r	Odd–even	Line (a)	A.D.I. (a)	Line (b)	A.D.I. (b)
0.1	7.884×10^{-4}	7.885×10^{-4}	8.107×10^{-4}	2.432×10^{-3}	2.432×10^{-3}
0.3	2.815×10^{-2}	2.815×10^{-2}	2.738×10^{-2}	3.488×10^{-3}	3.494×10^{-3}
0.6	1.353×10^{-1}	1.353×10^{-1}	1.316×10^{-1}	5.111×10^{-4}	3.451×10^{-4}
1.0	3.217×10^{-1}	3.216×10^{-1}	3.147×10^{-1}	4.150×10^{-3}	4.109×10^{-3}

TABLE V

Maximum Absolute Error at 10 Time Steps in the Thin Film

r	Odd–even	Line (a)	A.D.I. (a)	Line (b)	A.D.I. (b)
0.1	2.683×10^{-4}	4.949×10^{-4}	5.494×10^{-4}	1.529×10^{-3}	1.542×10^{-3}
0.3	1.785×10^{-2}	8.520×10^{-2}	1.634×10^{-2}	2.088×10^{-3}	2.290×10^{-3}
0.6	8.557×10^{-2}	1.777×10^{-2}	7.939×10^{-2}	5.116×10^{-4}	8.824×10^{-4}
1.0	2.023×10^{-1}	2.009×10^{-1}	1.900×10^{-1}	3.786×10^{-3}	2.385×10^{-3}

TABLE VI

Maximum Absolute Error at 20 Time Steps in the Thin Film

r	Odd–even	Line (a)	A.D.I. (a)	Line (b)	A.D.I. (b)
0.1	6.764×10^{-4}	8.429×10^{-4}	7.252×10^{-4}	2.522×10^{-3}	2.643×10^{-3}
0.3	1.597×10^{-2}	3.679×10^{-2}	1.656×10^{-2}	2.654×10^{-3}	2.802×10^{-3}
0.6	3.096×10^{-2}	1.775×10^{-2}	3.553×10^{-2}	1.329×10^{-3}	1.448×10^{-3}
1.0	8.884×10^{-3}	8.661×10^{-3}	8.324×10^{-3}	2.417×10^{-3}	2.340×10^{-3}

In order to ascertain the behavior of the hopscotch methods for the anisotropic problem we have used a theoretical solution once again. In this way the effect of aligning the implicitness parallel to or perpendicular to the direction of anisotropy is then apparent.

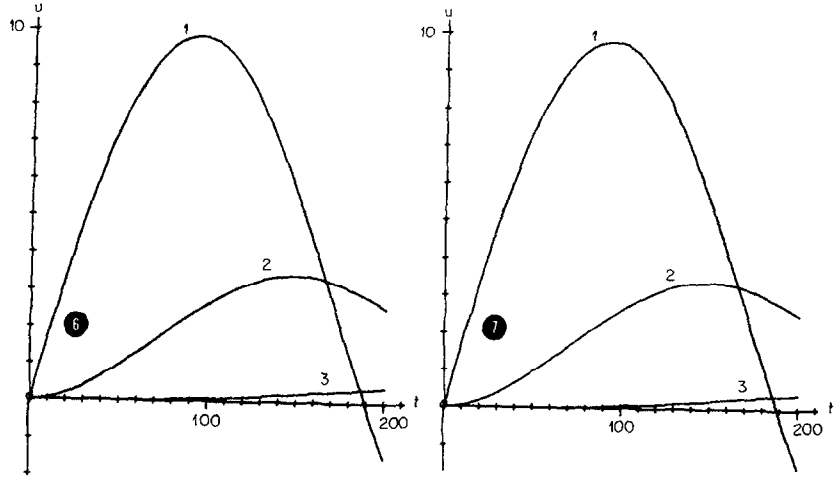

FIG. 6. Graphs of temperature distribution in an anisotropic thermal print element for a single switch off of the heat source; the solution obtained using the odd–even hopscotch algorithm.

FIG. 7. Graphs of temperature distribution in an anisotropic thermal print element for a single switch off of the heat source; the solution obtained using the perpendicular line hopscotch algorithm.

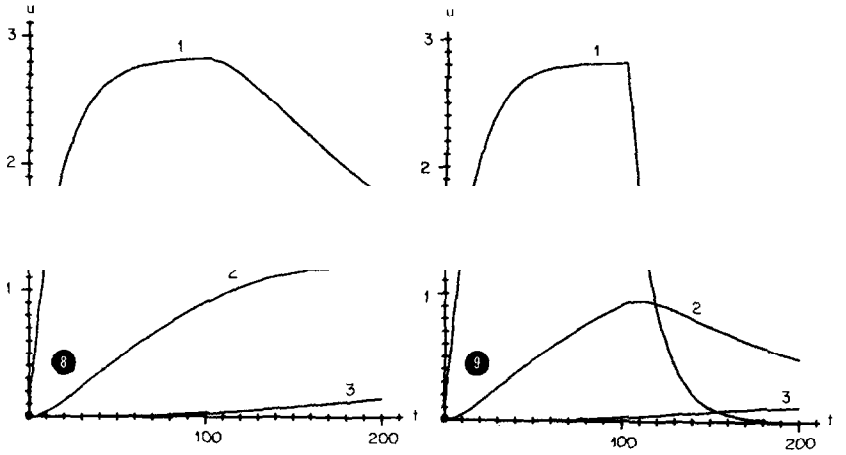

FIG. 8. Graphs of temperature distribution in an anisotropic thermal print element for a single switch off of the heat source; the solution obtained using the perpendicular A.D.I. hopscotch algorithm.

FIG. 9. Graphs of temperature distribution in an anisotropic thermal print element for a single switch off of the heat source; the solution obtained using the parallel line hopscotch algorithm.

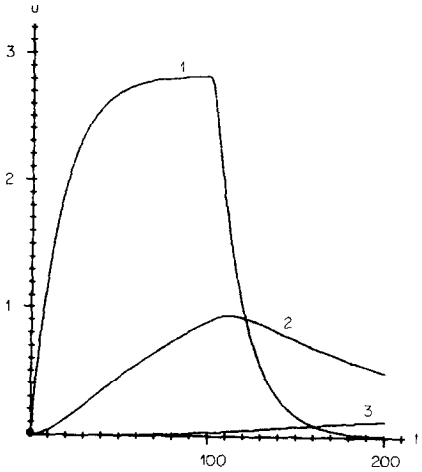

FIG. 10. Graphs of temperature distribution in an anisotropic thermal print element for a single switch off of the heat source; the solution obtained using the parallel A.D.I. hopscotch algorithm.

In Table IV it becomes clear that we must ensure the implicitness in the line and A.D.I. hopscotch methods coincides with the direction of anisotropy. Moreover, the results obtained by the odd–even hopscotch scheme are hopelessly inaccurate. These results clearly support our conjecture made in Section 3. We would surmise, therefore, that when applying our algorithms to the anisotropic problem with realistic physical data we would obtain significantly differing behaviors. To this end the anisotropic data $\alpha = 0, \beta = l = 1, h = 0.1, r = 1.0, \kappa_1 = 1.0, \kappa_2 = 100.0, \rho = 10.49, C = 0.0556, \kappa_3 = 0.0028, \kappa_4 = 0.28, \kappa_5 = 0.0028, \rho_1 = 2.4, C_1 = 0.2, h_0 = 0.000053, q = 10, u_\infty = 0.0, D = 0.000015$ with the initial temperature distribution $u(x, y, z, 0) = 0$, was employed and the results obtained using the hopscotch methods are reported graphically in Figs. 6–15. Figures 6–10 depict the temperature distribution in the print element computed by odd–even, perpendicular line and A.D.I., and parallel line and A.D.I. hopscotch algorithms, respectively, at the fixed points $\{x = y = 0.5, z = 0.0, 0.1, 0.3\}$ for a single switching of the heat source $t_0 = 100\tau$, and $0 \leqslant t \leqslant 200\tau$. A comparison of these shows that the parallel line and A.D.I. hopscotch methods produce physically realistic temperature distributions whereas the odd–even and perpendicular line and A.D.I. hopscotch methods work very poorly on the anisotropic problem. The contrast between the methods is even more dramatic when multiple switchings are effected as depicted in Figs. 11–15.

In Fig. 11, the odd–even hopscotch method has produced a distribution which has a rapid growth with no indication of a cooling period which exists when the heat

source is switched off. The same effect is apparent with the perpendicular line and A.D.I. methods as shown in Figs. 12 and 13, respectively. However, in using the parallel line and A.D.I. hopscotch methods, the cooling effect is apparent in Figs. 14 and 15 and the steady temperature pattern is obtained after approximately six cycles.

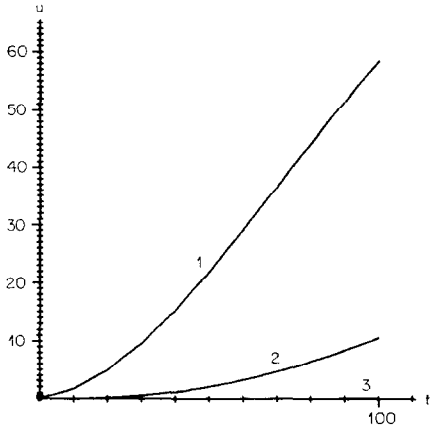

FIG. 11. Graphs of temperature distribution in an anisotropic print element for a print cycle of 10τ; the heat source being on for 5τ and off for 5τ—the odd–even hopscotch algorithm.

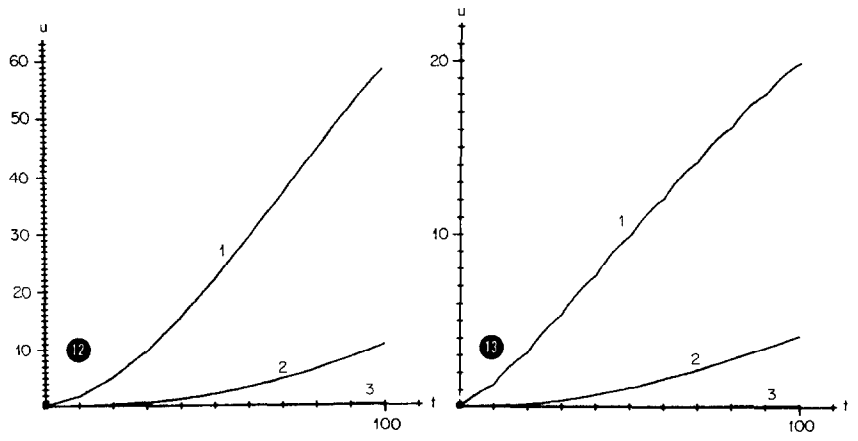

FIG. 12. Graphs of temperature distribution in an anisotropic print element for a print cycle of 10τ; the heat source being on for 5τ and off for 5τ — the perpendicular line hopscotch algorithm.

FIG. 13. Graphs of temperature distribution in an anisotropic print element for a print cycle of 10τ; the heat source being on for 5τ and off for 5τ — the perpendicular A.D.I. hopscotch algorithm.

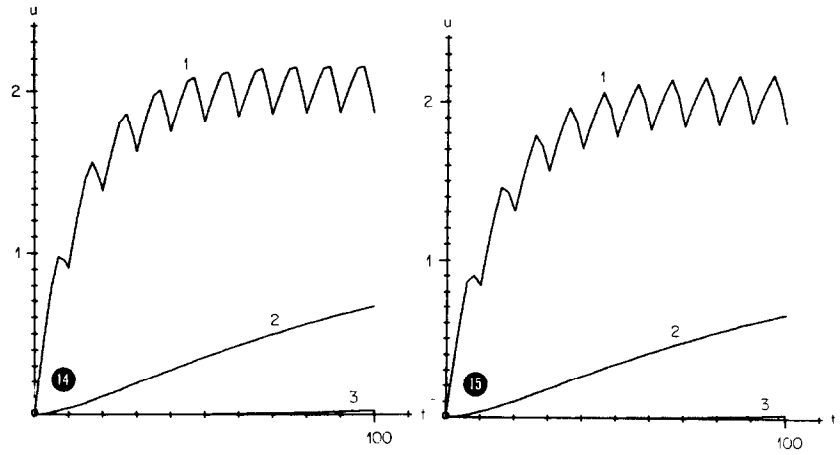

FIG. 14. Graphs of temperature distribution in an anisotropic print element for a print cycle of 10τ; the heat source being on for 5τ and off for 5τ — the parallel line hopscotch algorithm.

FIG. 15. Graphs of temperature distribution in an anisotropic print element for a print cycle of 10τ; the heat source being on for 5τ and off for 5τ — the parallel A.D.I. hopscotch algorithm.

From these latter figures the operating conditions for the thermal print head can be determined. That is, the highest peaks in Graphs (1) shown in Figs. 14 and 15 can be chosen so that this temperature is above that required for the chemical reaction to take place in the thermally sensative print paper; whereas, the lower troughs are chosen so that these points are below the critical temperature. We have chosen a heating cycle in which the heat source is on for the same amount of time as it is off, namely on for 5τ and off for 5τ. If the operating conditions are not satisfactory in practice (the troughs in Figs. 14 and 15 are not sufficiently low) then by adjusting the ratio of "on time" to "off time," so that a larger cooling time per heat cycle is effected, an appropriate cycle can be produced so that "smudging" of characters does not occur. For brevity we have omitted the figures illustrating this point.

5. Concluding Remarks

It can be concluded from Tables I–III that there is no *significant* difference in the accuracy of the results produced by the three hopscotch methods when applied to isotropic problems Eqs. (32) and (34). This result is further borne out by the results of the discontinuous heat source problem illustrated in Figs. 3–5. The odd–even hopscotch scheme, however, has a computational superiority over the line and A.D.I. hopscotch methods, as it does not require the solution of linear

sets of equations at each time step. The line and A.D.I. hopscotch methods, aligned in the x and y directions give the same results for isotropic problems.

The results in Tables IV–VI for the problems, anisotropic in the y direction, show that the odd–even, and the line and A.D.I. hopscotch schemes perpendicular to the anisotropy are completely inaccurate. In contrast the parallel line and A.D.I. hopscotch methods give a computational solution with three figure accuracy. Applying the line and A.D.I. hopscotch methods both in the x and y directions and the odd–even hopscotch scheme to a discontinuous heat source problem in an anisotropic medium, we see from the temperature distribution graphs for the five methods Figs. 6–10, that the low accuracy schemes give unrealistic results. The temperature distributions for a multiple switching of the heat source Figs. 11–15 again show the odd–even and perpendicular directional methods to be subject to a large error growth.

We conclude that for anisotropic problems that the use of the odd–even hopscotch method is not to be advocated and the line and A.D.I. hopscotch algorithms must be implemented in the direction of high anisotropy. Computationally, both methods are equivalent; however, the computing time required for the line hopscotch scheme is far less than that for the A.D.I. scheme for which there is no fast algorithm.

In all the numerical experiments the fast odd–even and fast line hopscotch algorithms were used whenever possible, i.e., when the solution was not required at every time step.

The computation was carried out on an Elliott 4130 computer at the University of Dundee.

Acknowledgments

Mr Nicoll's share of the work was carried out while he was in receipt of a University of Dundee research studentship.

References

1. L. K. Chen, Unsteady, three-dimensional, conductive heat transfer analysis of thin film composites, N.C.R. (Dayton) Report, June 1967.
2. C. K. Chu and G. Johansson, Numerical studies of the heat conduction equation with highly anisotropic tensor conductivity. II, Uppsala University, Dept. of Computer Sciences, Report No. 40, 1972.
3. C. K. Chu, K. W. Morton, and K. V. Roberts, Numerical studies of the heat conduction equation with highly anisotropic tensor conductivity, I, "Proceedings of 3rd International Symposium on Numerical Fluid Dynamics (Paris 1972)," Springer-Verlag, Berlin/New York, 1973.
4. P. Gordon, Nonsymmetric difference equations, *SIAM J. Appl. Math.* **13** (1965).

5. A. R. GOURLAY, A fast second order partial differential equation solver, *J. Inst. Math. Appl.* **6** (1970).
6. A. R. GOURLAY AND G. R. MCGUIRE, General hopscoth algorithms for the numerical solution of partial differential equations, *J. Inst. Math. Appl.* **7** (1971).
7. G. R. MCGUIRE, Masters Thesis, University of Dundee (1969).
8. A. R. MITCHELL, "Computational Methods in Partial Differential Equations," Wiley, New York, 1969.
9. J. LL. MORRIS, On the numerical solution of a heat equation associated with a thermal print head, *J. Comp. Phys.* **5** (1970).
10. J. LL. MORRIS, On the numerical solution of a heat equation associated with a thermal print head. II, *J. Comp. Phys.* **7** (1971).
11. J. W. WATTS, An iterative matrix solution method suitable for anisotropic problems, *Soc. Pet. Eng. J.* **11** (1971).
12. J. W. WATTS, A method for improving line successive overrelaxation in anisotropic problems—a theoretical analysis, *Soc. Pet. Eng. J.* **13** (1973).
13. V. K. SAUL'YEV, "Integration of Equations of the Parabolic Type by the Method of Nets," Pergamon, New York, 1964.